Available online at www.sciencedirect.com
ScienceDirect
International Journal of Heat and Mass Transfer 50 (2007) 1263–1268
International Journal of HEAT and MASS TRANSFER
www.elsevier.com/locate/ijhmt

A consideration on the relation between the oscillatory thermocapillary flow in a liquid bridge and the hydrothermal wave in a thin liquid layer

Hiroshi Kawamura *, Emi Tagaya, Yuta Hoshino

Department of Mechanical Engineering, Tokyo University of Science, 2641 Yamazaki, Noda-shi, Chiba 278-8510, Japan

Received 9 December 2005
Available online 18 December 2006

Abstract

The present study aims to establish relation between the hydrothermal wave (HW) in a thin liquid layer and the oscillatory flow in a half-zone liquid bridge with a small height to radius ratio. Numerical and experimental studies are performed on the HW in a liquid layer. Near the hot wall, the propagation direction of the HW is similar to that of the temperature traveling wave in the short liquid bridge. Thus, the oscillatory thermocapillary flow in the short liquid bridge should be interpreted to be closely similar to the HW appearing in the vicinity of the hot wall of the liquid layer.

Keywords: Thermocapillary convection; Hydrothermal wave; Liquid layer; Liquid bridge

1. Introduction

Smith and Davis [1] (SD hereafter) performed a linear stability analysis on a thermocapillary flow in an infinite liquid layer imposed by a constant-temperature gradient along a free surface. They have predicted a new instability in which an oblique temperature wave travels over the free surface with an inclined angle against the mean temperature gradient vector. The angle has been found to be dependent on the Prandtl number (Pr) of the fluid. It was named the hydrothermal wave (HW, hereafter). Afterwards, Riley and Neitzel [2] experimentally proved the existence of the HW. Their test section was a rectangular geometry with 30 and 50 mm in stream and spanwise lengths, respectively. The working fluid was silicone oil of 1 cSt. Xu and Zebib [3] made a numerical simulation on thermocapillary convection in a cavity including influence of sidewalls. They obtained a standing wave consisting of a pair of the HW. Burguete et al. [4] reported experiments on the buoyant thermocapillary instabilities with different aspect ratios for silicone oil of 0.65 cSt. They presented the critical Marangoni numbers and the nondimensional characteristics of the HW such as the frequency and the propagation angle for various depths and streamwise lengths.

On the other hand, it has been widely known [5] that the thermocapillary flow in a half-zone liquid bridge of a high Pr fluid exhibits the transition from the two-dimensional axisymmetric steady to the three-dimensional oscillatory flow with increasing temperature difference between the top and bottom surfaces. In the oscillatory flow, a thermal wave propagates over the free surface in the azimuthal direction.

These instabilities in the liquid layer and the liquid bridge have been found [6–8] originating from the common instability due to the HW because the temperature wave propagates over the free surfaces in both cases. It has been, however, not well recognized that a definite difference exists in their propagation angles. The present study aims to establish a relation between the HW in a thin liquid layer and the oscillatory Marangoni flow in a liquid bridge through a numerical simulation as well as an experimental observation.

* Corresponding author. Tel.: +81 471 24 1501; fax: +81 471 23 9814.
E-mail address: kawa@rs.noda.tus.ac.jp (H. Kawamura).

0017-9310/$ - see front matter © 2006 Elsevier Ltd. All rights reserved.
doi:10.1016/j.ijheatmasstransfer.2006.09.035

Nomenclature

b	temperature gradient, $-\mathrm{d}T/\mathrm{d}x$ (K/m)
c	specific heat (J/kg K)
c_R	phase speed
d	depth (mm)
k	wave number
L_x	streamwise length (mm)
L_z	spanwise length (mm)
Ma	Marangoni number, $Re \cdot Pr$
n	grid number
p	pressure (Pa)
Pr	Prandtl number, $\mu c/\lambda$
Re	Reynolds number, $\rho\gamma bd^2/\mu^2$
t	time (s)
T_{hot}	temperature at the hot wall (K)
T_{cold}	temperature at the cold wall (K)
ΔT	temperature difference, $T_{\mathrm{hot}} - T_{\mathrm{cold}}$ (K)
$\boldsymbol{v}$	velocity (u, v, w) (m/s)

Greek symbols

ϕ_A, ϕ_B	propagation angle (°)
γ	temperature coefficient of surface tension, $-\partial\sigma/\partial T$ (N/m K)
λ	thermal conductivity (W/m K)
μ	viscosity (Pa s)
θ	temperature difference, $T - T_{\mathrm{hot}}$ (K)
$\bar{\theta}$	mean value averaged over the spanwise direction (K)
θ'	temperature deviation, $\theta - \bar{\theta}$ (K)
ρ	density (kg/m^3)
σ	surface tension (N/m^2)

Subscripts

x, y, z	Cartesian coordinate
r, ψ, z	cylindrical coordinate

Superscript

$*$	quantity estimated with the temperature gradient in the central region

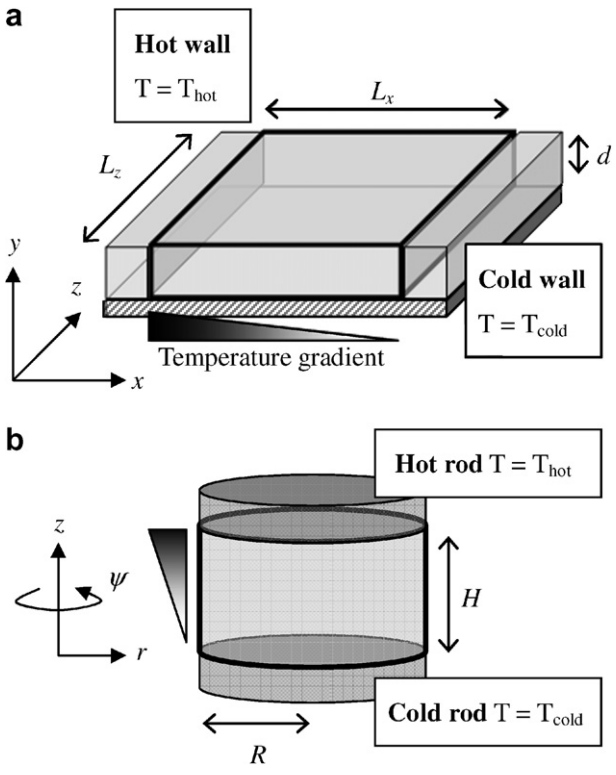

Fig. 1. Configurations of (a) liquid layer and (b) liquid bridge.

Configurations of the liquid layer and the liquid bridge in this study are shown in Fig. 1.

Note that an aspect ratio (=height/radius) of a liquid bridge which can be formed on the ground is limited to be smaller than about 1.0. Thus, the liquid bridge treated in the foregoing and the present studies are mostly with the aspect ratio equal to or less than 1.0.

2. Numerical simulation

The calculation is carried out for a liquid layer with a finite streamwise distance L_x and depth d. The hot and cold end walls are maintained at constant temperatures T_{hot} and T_{cold} with a difference of ΔT. The bottom and free surfaces are adiabatic. The non-slip condition is imposed on the end walls and the bottom surface. The periodic boundary condition is applied to the spanwise direction. The physical properties of the liquid are assumed constant except the surface tension. The test fluids are acetone ($Pr = 4.4$) and silicone oil of 0.65 cSt ($Pr = 10.3$). Since the results are similar for both fluids, the one with silicone oil of 0.65 cSt will be mainly described below.

The streamwise and spanwise lengths of the test section are $10d$ and $5\pi d$, respectively. The grid number ($n_x \times n_y \times n_z$) is $60 \times 20 \times 80$. We scale all distances on d. The velocity, pressure, temperature difference and time are scaled with $v_0 = \gamma bd/\mu$, $p_0 = \gamma b$, $\theta_0 = bd$ and $t_0 = \mu/\gamma b$, respectively.

The governing equations are the continuity equation

$$\nabla \cdot \boldsymbol{v} = 0, \tag{1}$$

the Navier–Stokes equation

$$Re\left(\frac{\partial \boldsymbol{v}}{\partial t} + (\boldsymbol{v}\cdot\nabla)\boldsymbol{v}\right) = -\nabla p + \nabla^2 \boldsymbol{v}, \tag{2}$$

and the energy equation

$$Ma\left(\frac{\partial \theta}{\partial t} + \boldsymbol{v}\cdot\nabla\theta\right) = \nabla^2\theta. \tag{3}$$

The boundary conditions over the free surface can be expressed as

$$\frac{\partial u}{\partial y} = -\frac{\partial \theta}{\partial x},$$
$$\frac{\partial w}{\partial y} = -\frac{\partial \theta}{\partial z},$$
$$v = 0.$$

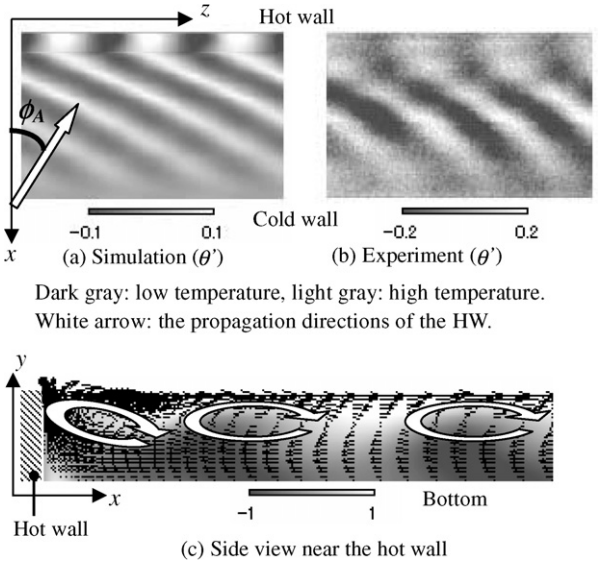

Fig. 2. Temperature contours and velocity vector in the HW.

3. Experimental setup

An experiment was also conducted, where a liquid layer was formed in a rectangular container. The bottom was made of Bakelite and the side walls are made of acrylic plate in order to approximate adiabatic boundary condition. The hot and cold end walls were manufactured with the brass. The hot wall was heated by a cartridge heater and the cold wall was cooled by the water. These hot and cold walls were able to provide uniform constant-temperature boundary condition, and were coated with a chemical to prevent wetting by liquid. The streamwise length of the test section was 10 mm, the spanwise 60 mm, and the depth 1 mm. We could measure the depth of the layer with micrometer to an accuracy of order of 0.01 mm. In this depth, thermocapillary convection was more dominant than buoyancy convection and we were able to observe almost pure HW according to Riley and Neitzel [2]. The test fluid was silicone oil of 1 cSt. We measured the surface temperature distribution with the infrared thermography and observed the x–y cross section flow field with the CCD camera.

4. Results and discussion

4.1. Hydrothermal wave in the liquid layer

In the numerical simulation, the HW instability emerges when the temperature difference exceeds a critical point. We usually obtained a standing wave at first. With elapse of the computation time, it changes to a traveling wave while ΔT is kept constant. The traveling temperature contour over the free surface is shown in Fig. 2(a) for $Ma = 1000$. The illustrated temperature contour is the temperature deviation θ'. Fig. 2(b) shows the temperature contour (θ') obtained by the experiment at $Ma = 654$. We can observe a similar oblique traveling wave also in the experiment.

As predicted by SD, the HW propagates from the cold to hot wall at an angle of ϕ_A with respect to the negative x-axis. Fig. 2(c) illustrates the velocity vector and the temperature contour in the vertical section. The temperature contour in this figure is the deviation from the mean temperature $\bar{\theta}^*(x)$, which is obtained by averaging $\bar{\theta}(x,y)$ over the y direction at each x. In the central region; i.e., the region outside the vicinity of the hot and cold walls, secondary multicellular vortices are superimposed upon

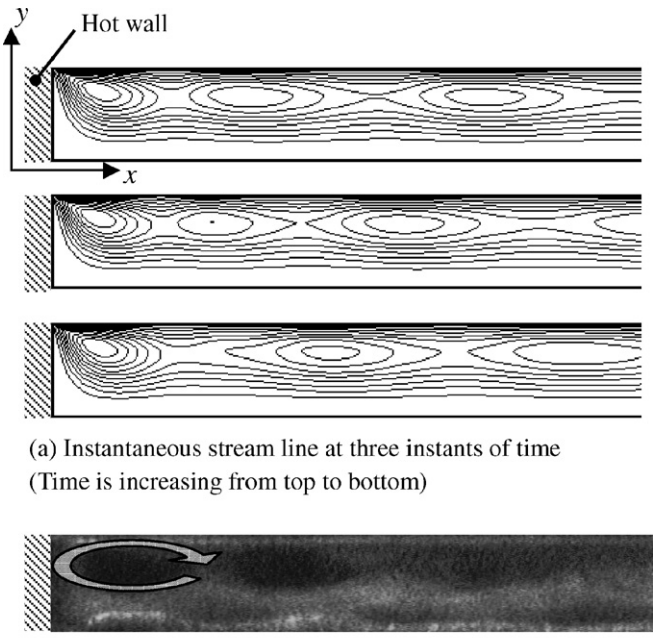

Fig. 3. Flow field in the liquid layer near the hot wall.

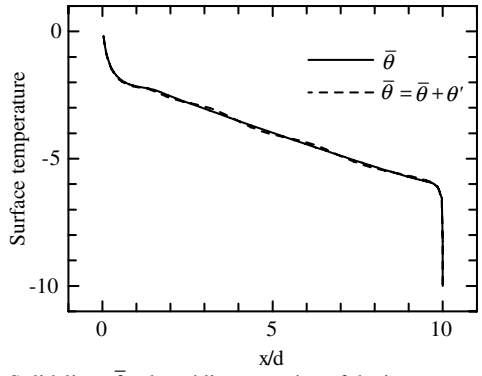

Solid line: $\bar{\theta}$, dotted line: snapshot of the instantaneous temperature θ'

Fig. 4. Temperature profile over the free surface.

the basic return flow [see Fig. 3(a)]. The secondary vortices rotate in the same direction as the basic return flow and are convected towards the hot wall. The axes of the circulations extend obliquely against the spanwise direction. The circulations cause a rolling up of cold fluid from the bottom side and let the oblique thermal wave propagate over the free surface. In contrast to these convected vortices, a vortex attached to the hot wall; i.e., the leftmost one in Figs. 2(c) and 3(a), is staying at the same position, although its size oscillates with the frequency of the HW. As seen in Fig. 3(b), stationary vortex was also observed on experiment.

The mean temperature $\bar{\theta}$ and a snapshot of the instantaneous one θ over the free surface are shown in Fig. 4. A steep temperature gradient is formed near the hot and cold walls, while an almost constant-temperature gradient is established in the central region.

4.2. Comparison with SD

We compare the obtained properties of the HW with the ones by SD. Note that the Ma is based on the mean temperature gradient b, while the actual temperature gradient in the central region of the liquid surface is smaller than the mean one (see Fig. 4). In the study of SD, they imposed a constant-temperature gradient along an infinite layer. Thus, to compare with SD, we define Ma^* using an obtained temperature gradient b^* in the central region. Then the present calculation corresponds to $Ma^* = 253$. Our calculation for $Pr = 10.3$ gives the propagation angle of $\phi_A = 37°$, the wave number of $k = 2.7$ and the phase speed of $c_R^* = 0.55$, while those by SD are $\phi_A = 33°$, $k = 2.5$ and $c_R = 0.58$ for the critical point of $Ma = 240$. Our results agree well with those by SD. An almost similar agreement was obtained for $Pr = 4.4$, too. Thus we can confirm the reliability of our calculation.

4.3. Temperature wave in the liquid bridge

For the liquid bridge, the temperature deviation on the unrolled free surface from the numerical simulation by the authors' group is presented in Fig. 5(a), numerical method is described in Ref. [9]. Fig. 5(b) illustrates the temperature contour and velocity vector in its vertical section. The aspect ratio (height to radius) is 1.0, the test fluid silicone oil of 2 cSt and $Ma = 40{,}000$, which is defined by the height of the liquid bridge and the temperature difference between the hot and cold ends. The mode number of the traveling wave is 2. Note that the wave propagates from the *hot to cold* surface at an angle of ϕ_B with respect to the negative x-axis, or almost parallel to the hot and cold ends. This propagation direction is quite different to the HW in the liquid layer, where the wave is directed from the *cold to hot* wall.

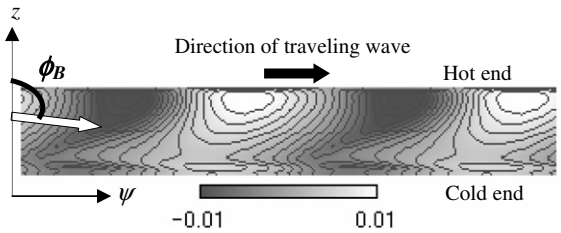

(a) Temperature deviation over the unrolled free surface.

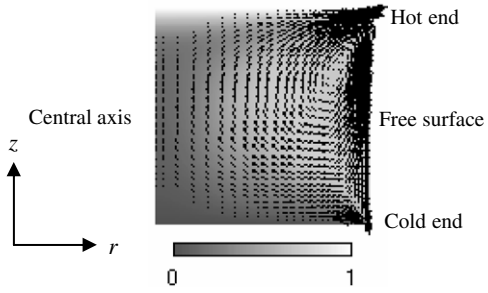

(b) Temperature contour and velocity vector in the vertical section.

Fig. 5. Temperature and velocity profiles of the traveling oscillatory flow in a liquid bridge with the height to the radius ratio of 1.0.

4.4. Bent HW near the hot wall in the liquid layer

To better understand the mechanism, we will pay an attention to the HW of the liquid layer not only in the central region but also in the vicinity of the hot wall. We have found that the front of the HW is bent near the hot wall as seen in Fig. 2(a) and (b). Fig. 6 enlarges this bent region. In this region, the steep temperature gradient is formed over the free surface due to the existence of the isothermal wall (see Fig. 4). Accordingly, a very high velocity is induced due to the thermocapillary force over the free surface near the hot wall region. As seen in Fig. 2(c), we can find a stationary vortex attached to the hot wall. The vortex causes a rolling up of a cold fluid returning along the bottom surface. The rolling up region extends to the distance of $1.3d$ in the x-direction. This distance is almost independent of Pr. A closer inspection reveals that the wave in this area propagates from the hot to cold wall at an angle of ϕ_A' with

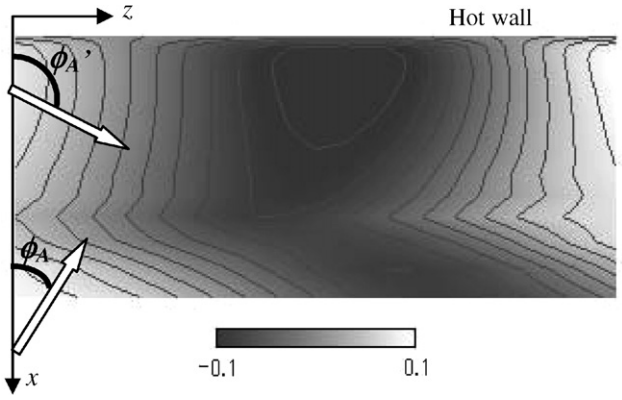

Fig. 6. Bent region of the HW near the hot wall.

respect to the negative x-axis. We can find also in the photograph of the experiment [Fig. 2(b)] that the propagation angle changes drastically in the vicinity of the hot wall.

We will discuss below the reason of the change in the propagation angle. Fig. 7 indicates the path lines of imaginary passive particles liberated from an isoline of the temperature wave traveling towards the hot wall. The vertical level of the liberation is selected as $0.25d$ from the bottom. Since the Pr is high, the temperature profile is almost frozen to the fluid. Thus, the traveling front of the temperature wave is well represented by the line of the particles released at the same time. Note that the particles impinge almost perpendicularly on the wall, while the temperature wave in the bottom region travels with an angle of ϕ_A. The temperature wave comes up to the free surface in the vicinity of the hot wall and travels along it with the reversed direction from the *hot to cold* wall. Thus, the angle of inclination on the free surface is also reversed as seen in

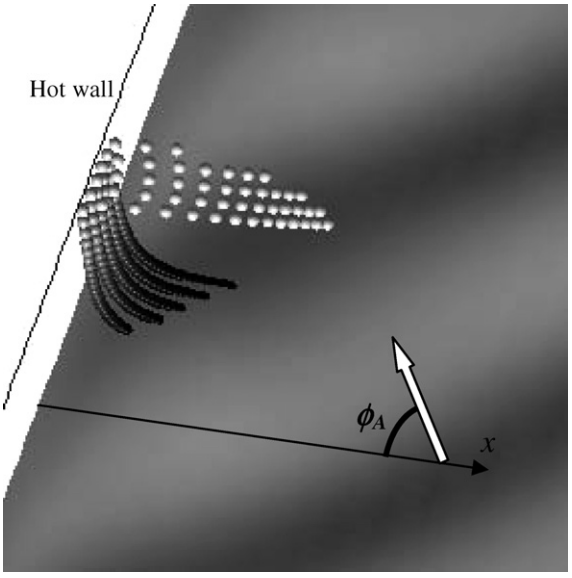

Fig. 7. Particle trajectory near the hot wall. The particles are librated from the isoline of the traveling wave at $0.25d$ from the bottom. Note that, after the impingement to the hot wall, the propagation angle of the wave is inversed over the free surface.

Fig. 7. If it is simply reversed at the hot wall, then the propagation angle over the free surface must be $\pi-\phi_A$. The obtained propagation angle ϕ_A', however, becomes more perpendicular to the x-axis, as seen in Fig. 6. The flow velocity in the hot wall vicinity is much larger over the free surface than in the bottom region (see Fig. 2(c)) because of the steep temperature gradient close to the hot wall (Fig. 4). This is the reason why the temperature contours near the hot wall is almost perpendicular to the hot wall; that is the traveling angle ϕ_A' is almost perpendicular to the x-axis.

4.5. Comparison with the liquid bridge

In the case of the liquid bridge with a small aspect ratio ($\leqslant 1$), a pronounced toroidal vortex as well as the azimuthally traveling wave exists as seen in Fig. 5(a) and (b). The traveling direction of the temperature wave over the free surface is almost perpendicular to the x-axis and is very close to that of the HW observed in the hot end region of the liquid layer [see Figs. 5(a) and 6]. The toroidal vortex appearing in the liquid bridge attaches stationarily to the hot end and oscillates with the frequency of the surface traveling wave. Thus, these facts strongly indicate that the traveling wave appearing in the thermocapillary flow of the liquid bridge is indeed driven by the HW, but it can be better interpreted by the close similarity to the hot end region of the HW in the thin liquid layer bounded by a finite domain between the hot and cold walls.

5. Conclusion

The temperature and flow fields of HW near the hot wall have been studied numerically and experimentally. A bent profile of the temperature wave is observed near the hot wall. The mechanism of the appearance of the bent profile is investigated, and the similarity to the traveling wave in the thermocapillary flow in a liquid bridge has been discussed. It was concluded that the traveling temperature wave appearing in the thermocapillary flow of the liquid bridge is driven by the HW, but it can be better interpreted by the close similarity to the hot end region of the HW in the thin liquid layer bounded by a finite domain between the hot and cold walls.

Acknowledgement

We would acknowledge Dr. I. Ueno at Tokyo University of Science for his contributions to preparation of the experiment.

References

[1] M.K. Smith, S.H. Davis, Instabilities of dynamic thermocapillary liquid layers. Part 1. Convective instabilities, J. Fluid Mech. 132 (1983) 119–144.

[2] R.J. Riley, G.P. Neitzel, Instability of thermocapillary-buoyancy convection in shallow layers. Part 1. Characterization of steady and oscillatory instabilities, J. Fluid Mech. 359 (1998) 143–164.

[3] J. Xu, A. Zebib, Oscillatory two- and three-dimensional thermocapillary convection, J. Fluid Mech. 364 (1998) 187–209.
[4] J. Burguete, N. Mukolobwiez, F. Daviaud, N. Garnier, A. Chiffaudel, Buoyant-thermocapillary instabilities in extended liquid layers subjected to a horizontal temperature gradient, Phys. Fluids 13 (10) (2001) 2773–2787.
[5] F. Preisser, D. Schwabe, A. Scharmann, Steady and oscillatory thermocapillary convection in liquid columns with free cylindrical surface, J. Fluid Mech. 126 (1983) 545–567.
[6] R. Velten, D. Schwabe, A. Scharmann, The periodic instability of thermocapillary convection in cylindrical liquid bridges, Phys. Fluids A 3 (2) (1991) 267–279.
[7] G.P. Neitzel, C.C. Law, D.F. Jankowski, H.D. Mittelmann, Energy stability of thermocapillary convection in a model of the float-zone crystal-growth process. Nonaxisymmetric disturbances, Phys. Fluids A 3 (12) (1991) 2841–2846.
[8] H.C. Kuhlmann, H.J. Rath, Hydrodynamic instabilities in cylindrical thermocapillary liquid bridges, J. Fluid Mech. 247 (1993) 247–274.
[9] M. Irikura, Y. Arakawa, I. Ueno, H. Kawamura, Effect of ambient fluid flow onset of oscillatory thermocapillary convection in half-zone liquid bridge microgravity, Sci. Technol. 16 (1) (2005) 176–180.